Integrative Biology

Accepted Manuscript

ROYAL SOCIETY OF CHEMISTRY

www.rsc.org/ibiology

Insights into Inhibition and Mechanism of Compounds against LPS-induced PGE_2 Production: a Pathway Network-based Approach and Molecular Dynamics Simulations

Xinzhuang Zhang,‡[1] Jiangyong Gu,‡[2] Liang Cao,[a] Yimin Ma,[a] Zhenzhen Su,[a] Fang Luo,[b] Zhenzhong Wang,[a] Na Li,[a] Gu Yuan,[b] Lirong Chen,*[b] Xiaojie Xu,*[b] Wei Xiao*[a]

Abstract

Comparing to current target-based screening approach, it is increasingly evident that active lead compounds based on disease-related phenotype are more likely translated to clinical trials in drug development. That is because human diseases are in essence the outcome of the abnormal function of multiple genes, especially complex diseases. Therefore, as an conventional technology in the early phase active lead compounds discovery, computational methods that could connect molecular interaction and disease-related phenotype to evaluate the efficacy of compounds are in urgent need. In this work, a computational approach by integrating molecular docking and pathway network analysis (network efficiency and network flux) was developed to evaluate the

[1] *State Key Laboratory of New-tech for Chinese Medicine Pharmaceutical Process, Kanion Pharmaceutical Corporation, Lianyungang City 222002, P.R.China. E-mail: xw_kanion@163.com (Wei Xiao); Tel: +86 0518 85521956*

[2] *Beijing National Laboratory for Molecular Sciences (BNLMS), State Key Laboratory of Rare Earth Materials Chemistry and Applications, College of Chemistry and Molecular Engineering, Peking University, Beijing 100871, P.R. China. E-mail: lirongchen@pku.edu.cn (Lirong Chen), xiaojxu@pku.edu.cn (Xiaojie Xu); Tel: +86 010 62757456*

† Electronic supplementary information (ESI) available.

‡ Contributed equally

efficacy of a compound against LPS-induced Prostaglandin E_2 (PGE_2) production. The predicted results were then validated *in vitro*, and the correlation with experimental results was analyzed by linear regression. In addition, molecular dynamics (MD) simulations were performed to explore the molecular mechanism of the most potent compounds. There were 12 hits out of 28 predicted ingredients separated from Reduning Injection (RDN). The predicted results had a good agreement with the experimental inhibitory potency (IC_{50}) (correlation coefficient = 0.80). The most potent compounds could target several proteins to regulate the pathway network. This might partly interpret the molecular mechanism of RDN on fever. Meanwhile, the good correlation of the computational model with wet experiments might bridge the gap between molecule-target interactions and phenotypic response, especially for multi-target compounds. Thus, it would be helpful for active lead compounds discovery and the understanding of the multiple targets and synergic essence of traditional Chinese medicine (TCM).

Keywords

Pathway network; Reduning Injection; network efficiency; network flux; LPS-induced PGE_2 production;

1 Introduction

During the last 20 years, the approved drugs did not increase significantly, although more cost and new technologies (such as combinatorial chemistry, high-throughput screening, -omics)[1] were applied to discover more candidate molecules and new targets in drug development. It should be to some extent attributed to the current

drug-development paradigm, and the "one drug-one target" paradigm made it difficult to translate the in vitro activity to a desire clinical effect owing to ignoring the systematic information[2]. Whereas, as a renewed drug discovery strategies, phenotypic screens are applied to measure the desired biological effect of a molecule on cells, tissues or whole organisms even if the molecular mechanism and protein targets are unclear. Moreover, the phenotypic approache was confirmed to translated the active lead compounds to the approved drugs more effectively[3]. Thus, it was gradually paid close attention by pharmaceutical industry and academic research centers[4].

As an essential method to identify lead compounds, computational techniques played an important role in observing interactions between small molecules and proteins, and reduced amount of experimental works[5]. Along with the development of systems pharmacology and network analysis, some computational approaches at the systems level were explored to improve the successful rate of the drug development. Pathways were the underlying biology of diseases[6], and could connect individual molecular components to disease-related phenotypes by functional protein networks[7]. Thus, biological pathways were generally considered to be partially phenotypic[8, 9]. According to the above concepts[10-12], a compoutational model integrating biological pathway and network analysis was developed to evaluate the efficacy. It might also be applied to discover lead compounds and interpret the molecular mechanism.

It has long been known that Prostaglandin E_2 (PGE_2) was the principal inflammation mediator, which participated in several pathological processes such as fever, sickness behaviors, and inflammatory pain[13-15]. Moreover, the febrile response

is accompanid by the significant increase of both peripheal and central of PGE2[13, 16]. Reduning Injection (RDN) was a Chinese medicine prescription which was composed of *Lonicerae Japonicae* Flos, *Gardeniae Fructus* and *Artemisiae Annuae* Herba. It has been widely used in China to alleviate or treat the symptoms of upper respiratory tract infections (URTIs), especially the fever days and severity[17-19]. Thus, a pathway network of LPS-induced PGE_2 production was constructed, and was applied to identify active compounds and to explore the potential molecular mechanism on fever. The results showed that the computational approach integrating pathway network and molecular docking, could effectively translate the predicted compounds of virtual screening to wet experiments. Meanwhile, it might also bridge the gap between molecular details and disease-related phenotypes, and provide an alternative way to discover lead compounds in early-phase drug discovery.

2 Methods

2.1 Pathway network construction

A pathway network of LPS induced PGE_2 production (Figure 1) was constructed by integrating reported literatures[20-27] and pathway databases (such as Reactome[28] and KEGG[29]), which contained 30 nodes and 38 edges (arrows). In the directed network, Nodes were proteins or small molecules, and arrows corresponded to connectivity relationships among cellular elements. The direction of the arrows implied that the latter (node) was regulated by the former.

2.2 Molecular docking

In the pathway network, there were fourteen proteins (Table 1) which had reported

structures. Their complex structures (crystal or NMR) were obtained from RCSB Protein Data Bank (http://www.pdb.org/) for molecular docking. For the protein structures, water molecules and ligands were removed, the polar hydrogens were added and Kollman united atom partial charges were assigned by the Hydrogen module in AutoDock Tools (ADT). The docking was then performed by AutoDock 4.0.1 program in DOVIS 2.0 suite[30, 31]. The energy grid maps of docking simulation were established by a 10×10×10 Å cube and centered on the occupied space of the original ligand with a spacing of 0.375 Å between the grid points. The following ligand conformations in the active site were sampled by the Larmarckian genetic algorithm. The parameters were listed as follows: population size was set to 150, maximum number of energy evaluations to 2.5×10^7. Twenty independent docking runs were performed for each ligand, and the results were clustered according to the root mean square deviation tolerance of 2.0 Å. Other parameters were default. The original ligands or known inhibitors were chosen to determine the affinity of a compound to the corresponding protein target. The ligand library for molecular docking contained 90 natural products separated from RDN[32, 33].

Table 1. Fourteen target proteins of the pathway network of LPS-induced PGE_2 production for molecular docking

Protein	Protein name	UniProt	PDB	Ligand
TLR4	Toll-like receptor 4	O00206	4G8A	4G8A
PGES	Prostaglandin E synthase	O14684	3DWW	3DWW
TAK1	Mitogen-activated protein kinase kinase kinase	O43318	2YIY	2YIY
AP-1	Transcription factor AP-1	P05412	1FOS	Curcumin(keto)[a]
IκBα	Nuclear factor-kappa-B	P19838	3GUT	Caffeic acid

	p105 subunit			phenethyl ester [a]
ERK1	Mitogen-activated protein kinase 3	P27361	2ZOQ	2ZOQ
COX-2	Prostaglandin G/H synthase 2	P35354 [b]	3LN1	3LN1
JNK	c-Jun N-terminal kinase	P45983	3PZE	3PZE
MKK4	mitogen-activated protein kinase kinase 4	P45985	3ALN	3ALN
MKK6	mitogen-activated protein kinase kinase 6	P52564	3FME	3FME
p38	Mitogen-activated protein kinase 12	P53778	1CM8	1CM8
MEK1	mitogen-activated protein kinase kinase 1	Q02750	3DY7	3DY7
TRAF6:RIP1	Receptor-interacting serine/threonine-protein kinase 1	Q13546	4ITJ	4ITJ
TRAF6	TNF receptor-associated factor 6	Q9Y4K3	1LB5	TRAF6-binding peptide

[a] the original ligands of the two proteins were two known inhibitors according to the reported literatures[34, 35], and their two-dimensional structures were listed supplement Figure S1.

[b] the crystal structure of mouse COX-2 (UniProt ID: Q05769) based on blast analysis of the sequence with human COX-2 (UniProt ID: P35354) were selected for molecular docking, and the rest were human origins.

2.3 Calculation of network efficiency and network flux

The influence of a compound on a network depended on the docking scores between the compound and corresponding protein targets. We assumed that a compound with higher docking score would have more strongly inhibitory activity on a protein target. For every target, the ligand with highest binding energy was defined as the reference, and could inhibit the protein target by 99.5%. The initial value of the edges in the

network was set as 1. Thus, the reference ligand made the value of the edges that came out of the protein target up to 200. For other ligands, the values of all direct downstream edges of the target were calculated by the following expression:

$$EV = 10^{\left(Score_{liga} \quad /score_{reference}\right)\times 2.30} \ldots\ldots\ldots\ldots\ldots\ldots (1)$$

Where $score_{\text{reference}}$ and $score_{\text{ligand}}$ represented the docking score of the reference ligand and other compounds, respectively, and *EV* was the edge value of the arrow that came out of the target in the network.

When a network was attacked by a compound, its influence on the network was quantified by network efficiency (*NE*) which was the sum of the reciprocals of the shortest path length between all pairs of nodes[36]. Therefore, the metric was also applied to evaluate the efficacy of multi-target drugs[11, 12, 37].

$$NE = \sum_{i\neq j\in G} \frac{1}{d_{ij}} \ldots\ldots\ldots\ldots\ldots\ldots\ldots\ldots\ldots\ldots\ldots\ldots\ldots\ldots (2)$$

Where d_{ij} was the shortest path between nodes *i* and *j* of the network. If it was a directed and weighted network, d_{ij} was the shortest directed path with a minimum weight. To give a relative value, the quantity of *NE* was divided by *NE* of a fully connected state (NE_{max}, all *EV*s were set to 1), and the percentage of *NE* decrease (*NEd*) for an attack was defined as follow:

$$NEd(\%) = \frac{NE_{max} - NE_{attack}}{NE_{max}} \times 100 \ldots\ldots\ldots\ldots\ldots (3)$$

Where NE_{attack} was *NE* of *G* for an attack.

Generally, the downstream protein would be more important according to information flow model in a pathway network[38, 39], which was not reflected by *NE*. Therefore, network flux (*NF*) was introduced to weight *NE*[12], and *NF* was calculated

by the following equation:

$$NF = \sum_{i \neq j \in G, j=exit} \frac{1}{d_{ij}} \ldots\ldots\ldots\ldots\ldots\ldots\ldots\ldots\ldots\ldots\ldots\ldots (4)$$

Where the node *j* represented the exit of graph *G*, and d_{ij} was the shortest path from nodes *i* to nodes *j*. And the percentage of *NF* decrease (*NFd*) of the network for an attack was calculated by the following equation:

$$NFd(\%) = \frac{NF_{max} - NF_{attack}}{NF_{max}} \ldots\ldots\ldots\ldots\ldots\ldots\ldots\ldots (5)$$

Where NF_{max} represented *NF* of a fully connected state (all *EVs* was 1), and NF_{attack} was *NF* of *G* when it was attacked.

Finally, combination of *NE* and *NF* (*NEF*), a metric of the influence on a network for an attack, was defined as the square root of the product between *NEd* and *NFd*.

$$NEF(\%) = \sqrt{NEd \times NFd} \ldots\ldots\ldots\ldots\ldots\ldots\ldots\ldots\ldots (6)$$

NE and *NF* were calculated according to the redefined edge values by a program written in C++ language using Dijkstra Algorithm when a compound attacked a netowrk[12]. The interference of the compound on the pathway network was then characterized by *NEF*, and the higher the index was, the more strong it had inhibitory activity on PGE_2.

2.4 Experimental validation

The inhibitory activities of these compounds against PGE_2 production were determined by Prostaglandin E_2 EIA kit (Enzo Life Sciences, Farmingdale, NY, USA) *in vitro*. First, murine macrophage RAW264.7 cells (Cell Culture Center of the Chinese Academy of Medical Sciences, Beijing, China) were cultured in high-glucose Dulbecco's Modified Eagle's medium (DMEM, Gibco, Carlsbad, USA) supplemented

with penicillin (100 U/ml), streptomycin (100 μg/ml) and 10% (v/v) fetal bovine serum (FBS, Sijiqing, Deqing, Hangzhou, China) at 37° C containing 5% CO_2. Second, the influence of these compounds on cell viabilities were determined by 3-(4, 5-dimethylthiazol-2-yl)-2, 5-diphenyl tetrazolium bromide (MTT) methods. In 96-well plates, 4×10^4/well Cells were seeded for 24h, and then incubated by various concentrations of these compounds for another 24h. Then, 10 μl of MTT working solution (5 mg/ml) was added to each well, and the cells were incubated for another 4h at 37 ℃. After adding to 150 μl of DMSO, the absorbance at 490nm was measured using SpectraMax M2e Microplate Reader (Molecular Devices, Menlo Park, USA). Third, the cells were plated in 24-well culture plates (1×10^5 /ml) for 24h at 37 ℃, and were then treated with various concentrations of these compounds or positive drug (Celecoxib) for 1h, followed by 16~18h stimulation with LPS (1 μg/ml). Finally, the supernatants were diluted 5 times with FBS-free DMEM and the levels of PGE_2 were determined according to the manufacturer's protocol. The inhibitory potency (IC_{50}) of the compound was calculated by GraphPad Prism 5.0 (Table 2).

2.5 MD simulations

MD simulations in this work were performed by using the AMBER 11 simulation package, as decribed previously[40]. In brief, every compound-target complex was solvated in a truncated octahedral water box of TIP3P before energetically minimized using 2500 steps of Steepest Descent and 2500 steps of Conjugate Gradient method. The system was then heated gradually from 0 to 310 K without constraint for 60 ps, and equilibrated for another 60 ps in 310 K. The simulation was performed for 10 ns

in the NVT ensemble with snapshots save at every 1.0 ps. The time step was set to 2 fs. Particle Mesh Ewald (PME) was employed for electrostatic calculation, and the SHAKE method was used to constraint bonds containing hydrogen atoms.

3 Results and Discussion

3.1 Pathway network Analysis

The global topology analysis of the pathway network of LPS-induced PGE_2 production (Figure 1) was performed by NetworkAnalyzer, a plugin of Cytoscape 2.8.1[41]. The connectivity distribution was $P(k)=21.235 \times k^{-2.382}$ (out-degree distribution, r = 0.95), and the average shortest path length was 4.36. This showed that the biological network had typical scale-free and small-world properties, and had strong network robustness and information transmission[42, 43]. The result also implied that the pathway network had the ability to maintain stable phenotypes when it was attacked[44, 45].

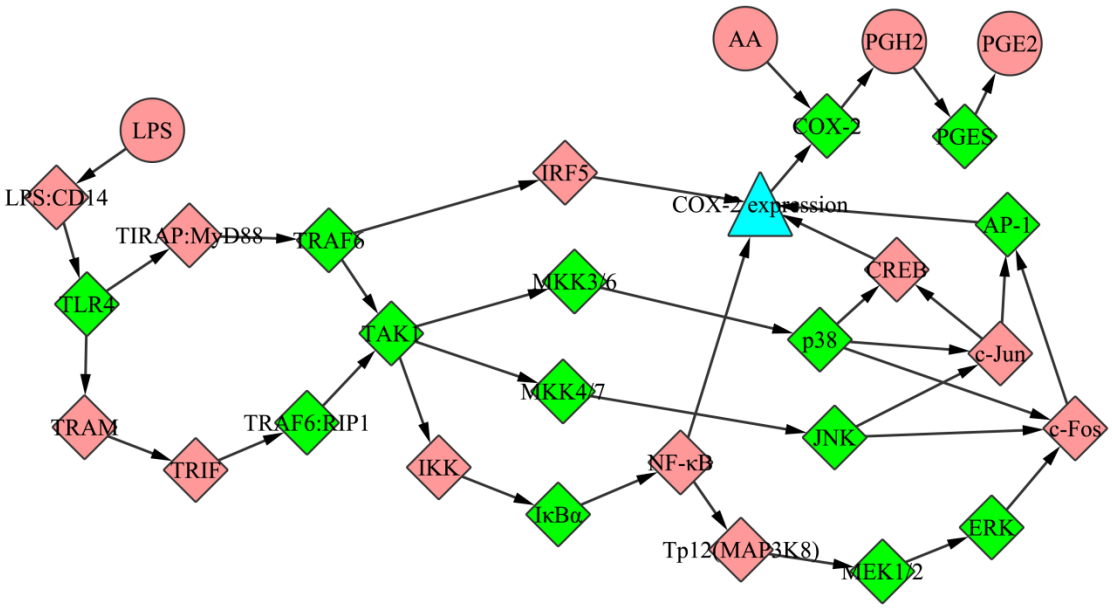

Figure 1. Pathway Network of LPS-induced PGE_2 production. Diamond and ellipse represented proteins and molecules, respectively. Green diamond represented the

target proteins for molecular docking.

3.2 Pathway network-based active compounds screening and validation

In the pathway network, seven target proteins with high betweenness would play more important roles in mediating signal transduction[46, 47], so they were selected and fully knocked out. The results showed that comparing with the fully connected state, *NE* of the whole systems dropped from 11.48 to 3.45. It was similar to the other connected state that the 14 docking protein targets were fully knocked (*NE* was 1.75). In constrast to the multi-target state, the pathway network had slight change when one protein target with high betweenness was blocked. Therefore, *NE* was considered to effectively measure the damage of pathway network when it was attacked.

NE could reflect the alternation of a network after an attack, thus it was also applied to assess the efficacy of a compound at cellular or organism level[12, 37, 48]. For each compound, *NE* was calculated according to docking scores between the compound and 14 protein targets in the pathway network. Of the molecules with high *NE*, 28 compounds (Figure S1) were available to purchase, and the inhibitory activities against PGE_2 production were determined in RAW264.7 cells. The primary assays (500 μM) showed that there were 15 compounds with strong inhibitory activities (over 50%). The further assays also verified the inhibitory activities of 12 compounds with various concentrations (Table 2). In the active compounds, five ingredients had strong activities with IC_{50} less than 40 μM. Luteolin, isorhamnetin and caffeic acid almost completely blocked PGE_2 production at the concentration of 62.5 μM. In addition, most compounds had the inhibitory activity over 50% at the

concentration of 125 μM (Table 2). The result implied that the hit rate was 42.86%, and the approach might improve the success rates from virtual screening at molecular level to wet experiments.

Table 2. Predicted potency and experimental results of each compound against LPS-induced PGE_2 production

Compound	IC_{50} (μM)	Inhibition[a]	*NEd* (%)	*NFd* (%)	*NEF* (%)
Scopoletin	38.46	0.77	37.01	57.41	46.10
Luteolin	2.565	ND[b]	50.33	58.00	54.03
Ferulic acid	128.0	0.51	33.50	78.74	51.36
Quercetin	51.84	0.64	44.13	56.85	50.09
Caffeic acid	17.35	0.88	32.63	70.33	47.91
Neochlorogenic acid	371.6	0.33	34.41	22.60	27.89
Artemisinin	25.57	0.84	60.27	80.05	69.46
Geraniol	100.8	0.52	19.81	29.54	24.19
Isorhamnetin	11.30	ND[b]	41.30	49.68	45.29
Isochlorogenic acid A	623.3	0.29	7.89	2.05	4.02
Coumarin	49.14	0.65	34.61	54.86	43.57
Protocatechuic acid	46.34	0.60	29.65	55.20	40.45

[a] The inhibition effect was determined in the final concentration of 125 μM.

[b] ND represents not data due to the influence of the compound with 125 μM concentration on cell viability.

As the most successful drug target class in the pharmaceutical industry, the interaction between G-protein-coupled receptors (GPCRs) and their extracellular ligands has proven to be an attractive point of interference for therapeutic agents[49]. PGE_2, a metabolite from arachidonic acid (AA), participated in several biological process through four distinct GPCRs (EP1, EP2, EP3, and EP4) such as fever,

sickness behaviors, mucosal integrity, inflammation and pain[50, 51]. Therefore, the blockade of PGE_2 synthesis would also effectively regulate the GPCR downstream signaling to improve the above symptoms. Among the active compounds against the release of PGE_2, luteolin, isorhamnetin, quercetin belonged to flavonoids, and the comparison of the activities of the three molecules indicated that 3`-OH and 3-OH could obviously decrease inhibitory activity. There were five compounds (caffeic acid, ferulic acid, neochlorogenic acid, isochlorogenic acid A, protocatechuic acid) which belonged to smaller polyphenolic molecules and contained an essential structural element (caffeic acid) in common. The contrast of the effect of these compounds confirmed that the two hydroxy groups in the 3 and 4 positions of the caffeic acid were important to their activities, but the presence of quinic acid remarkably reduced the effect. Scopoletin and coumarin, which both contained an essential structure of coumarin core, displayed moderate activity against PGE_2 production. This understanding relating the chemical structure of these active compounds would facilitate the design of compounds with higher potency against PGE_2 production, and provide important information for drug discovery from flavonoids, polyphenolic compounds and coumarin.

In order to investigate the quantitative relationship between predicted potency of and the experimental inhibitory potency, linear regression was employed to analyze the correlation. The result revealed that comparing with *NEd* (r = 0.60) (Figure 2A), the correlation coefficient of *NEF* with inhibitory rate at the concentration of 125 μM was increased to 0.77 after integrating the importance of the downstream nodes

in the pathway network (Figure 2C). Moreover, there was also a good correlation between the experimental inhibitory potency (IC_{50}) and *NEd* or *NEF*, and the correlation coefficients were 0.62 and 0.80, respectively (Figure 3A and 3C). Thus, it was showed that the method could not only effectively distinguish active compounds against LPS-induced PGE_2 production from complex systems (such as Traditional Chinese medicine), but also quantitatively predict the efficacy (IC_{50}) of the multi-target compounds by the linear regression equation (Figure 3C). In addition, the result also implied that the computational model combining molecular docking, biological pathway, and network analysis might simulate drug-induced phenotype response at cellular level.

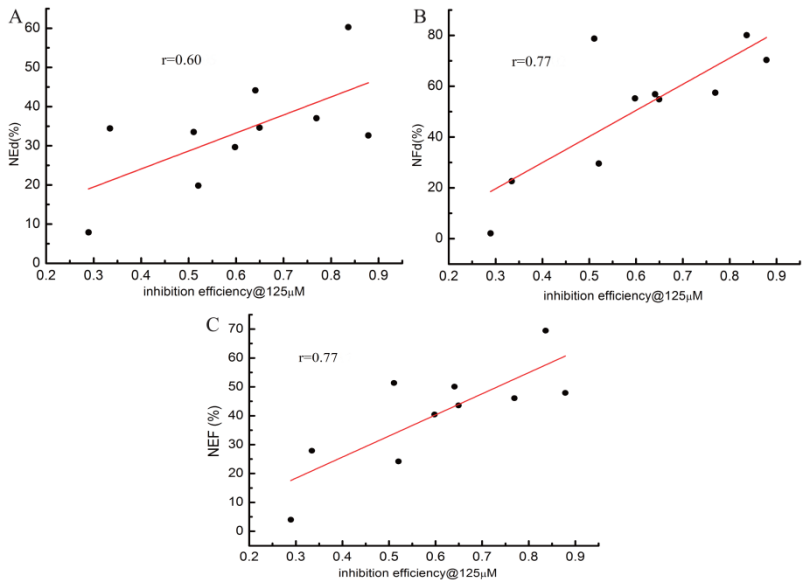

Figure 2. Experimental inhibition activity *vs* predicated potency: network efficiency (A), network flux (B), combination of network efficiency and network flux (C).

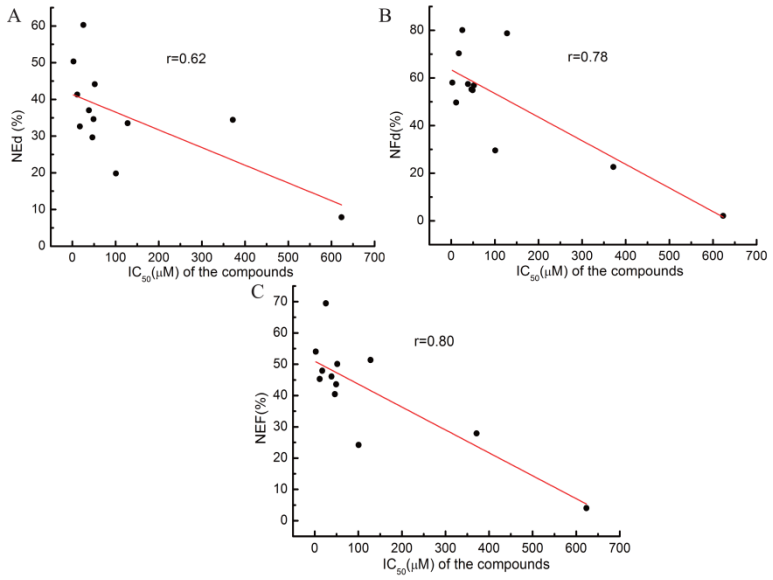

Figure 3. Experimental inhibitory potency (IC_{50}) *vs*. predicated potency: network efficiency (A), network flux (B), combination of network efficiency and network flux (C).

3.3 Comparison with target-based screening

According to the above results, it seemed reasonable to infer that pathway-guided virtual screening could identify active lead compounds, especially multi-target molecules. To further explore the computational methods, we compared pathway network-based screening with target-based screening. In the pathway of PGE_2 production, it has been widely known that COX-2 and PGES were limiting-rate enzymes, and drugs targeted the two protein could directly inhibit PGE_2 production[13, 52]. Their *NEF* were higher than that of other nodes (32.74% and 22.47%), when the two nodes were fully blocked, respectively. The experimental result also confirmed that the PGE_2 was completely inhibited by the approved drug Celecoxib (a selective COX-2 inhibitor) [14] at the concentration of 3.3 μM. But the correlation coefficients between experimental potency (IC_{50}) and the predicted potency (docking score or the

accurate binding free energy) were very bad (0.19 and 0.69, 0.28 and 0.049) for the compounds interacting with COX-2 or PGES (score was no less than 0). The results indicated that the computational approach could translate the interactions at molecular level to the desired effect, and also efficiently evaluate the activity of multi-target compounds. Thus, the method might be helpful to cell-based phenotypic screeing in drug discovery.

3.4 Molecular dynamics (MD) simulations

MD simulations could more accurately calculate the binding affinities through the flexibility of protein and ligand, thus it has been widely applied to simulate the interaction between active compound and protein target[53]. In this work, MD was performed to investigate the interactions between three active molecules (artemisinin, scopoletin and caffeic acid) and the corresponding targets in the pathway network. The compounds were subjected to 10 ns MD simulations, and the binding free energies of the snapshots of the last 3 ns trajectory were then listed in Table 3. Trajectory analysis was showed to have low fluctuation after 7 ns (Figure S2). The results showed that the compounds had strong interaction with many protein targets, which was confirmed by some reported literatures. For example, scopoletin could inhibit the phosphorylation of p38, ERK and JNK in concentration dependent manner, and caffeic acid could inhibit the phosphorylation of JNK, MKK4/7 and TAK1[54, 55]. The protein targets of mitogen-activated protein kinases (MAPKs) family also played an important role in regulating the production of pro-inflammatory cytokines (such as PGE_2), and some were known as drug targets for new anti-inflammatory drugs

development[56]. Thus, it might interpret the molecular mechanism of RDN against fever.

The binding modes for three protein-ligand complex conformations were showed in Figure 4. For MKK4 protein (PDB code: 3ALN), scopoletin was surrounded by hydrophobic residues Leu154, Ile26 and Val34, and formed hydrogen bonds with Met99, Arg28, Lys105 residue in the active site (Figure 4A). The interaction between TAK1 (PDB code: 2YIY) and caffeic acid might be hydrophobic, Pi-pi interaction between phenyl ring of ligand and hydrophobic residues (such as Val20, Phe146 and Leu133), as well as hydrogen bonds between hydroxyl oxygen atom and nitrogen atoms in Glu47, Ala77 residues (Figure 4B). Figure 4C showed that artemisinin could interact with PGES (PDB code: 3DWW) by hydrophobic-hydrophobic interactions between phenyl ring of ligand and the residues of binding cavity (eg. Thr166, His204, Leu201). The binding modes of the other top six protein-ligand complex conformations were listed in Figure S3.

Table 3. Binding free energies ($\triangle G_{bind}$/kcal.mol^{-1}) between active molecules and 14 target proteins

Protein	PDB	Scopoletin	Caffeic acid	Artemisinin
TRAF6:RIP1	4ITJ	-23.18	-18.12	-30.55
MKK4	3ALN	-22.80	-12.51	-23.09
MKK6	3VN9	-20.28	-13.55	-22.01
TAK1	2YIY	-20.20	-17.61	-21.07
JNK	3PZE	-19.21	-9.06	-14.97
COX-2	3LN1	-19.18	-14.39	-24.00
ERK1	2ZOQ	-19.06	-15.43	-20.28
IκB α	3GUT	-18.80	-15.3	-17.77

TLR4	4G8A	-18.56	-9.11	-29.85
PGES	3DWW	-16.79	-17.83	-27.72
AP-1	1FOS	-17.78	-13.12	-11.25
p38	1CM8	-13.83	-13.39	-19.49
MEK1	3DY7	-16.15	-12.86	-14.14
TRAF6	1LB5	-11.19	-8.72	-17.15

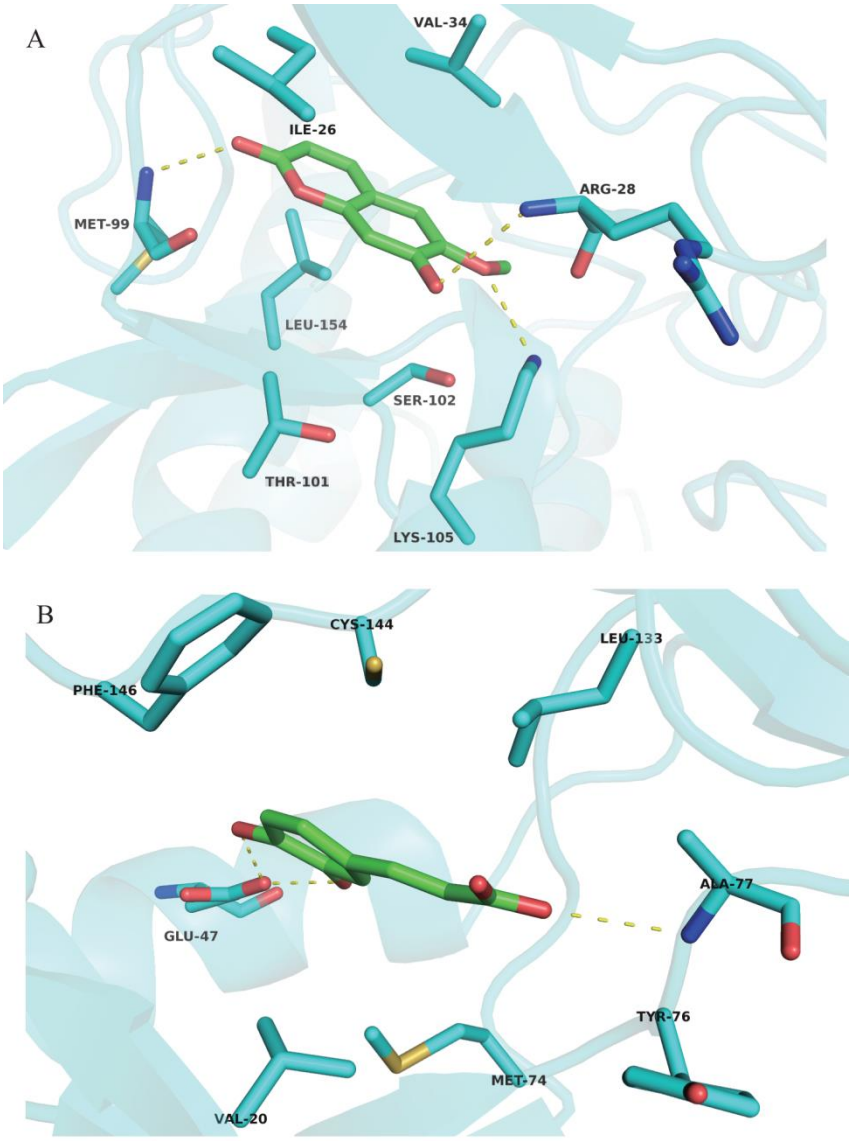

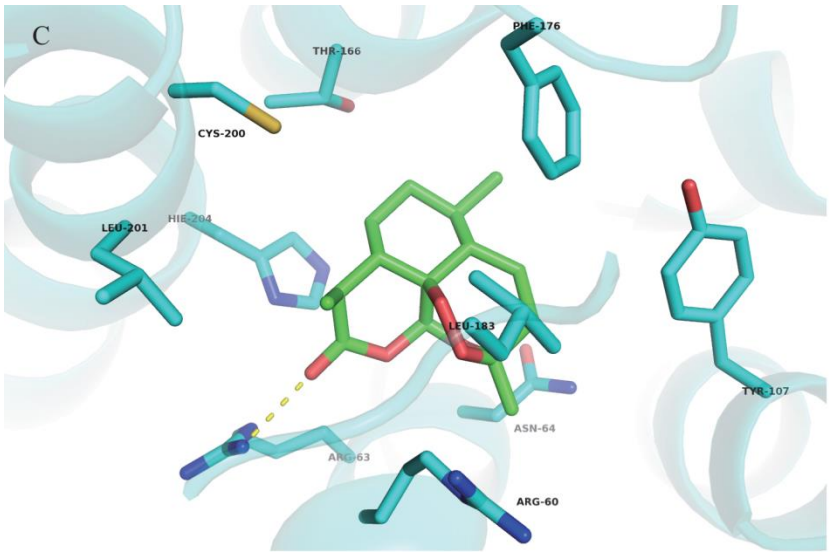

Figure 4. The binding modes of (A) complex scopoletin/MKK4 (3ALN), (B) complex caffeic acid/TAK1 (2YIY) and (C) complex artemisinin/PGES (3DWW) after 10 ns MD simulations. Ligands and some important residues were showed in stick, and hydrogen bonds were showed in dashed line (yellow). The RMSDs of their complexes were showed in Figure S2. See also Figure S3 for the binding modes of the other protein-ligand complexes.

4 Conclusions

A recent trend for active lead compounds discovery was to move toward systems-oriented approaches such as phenotypic assays and computational methods. In this work, first, combination with molecular docking and pathway network analysis was applied to interpret the molecular mechanism of RDN against LPS-induced PGE_2 production, which would provide a novel opportunity to illustrate the mechanism of traditional Chinese medicine (TCM). Second, the correlation with experimental results showed that the approach could offer an efficient way to identify active compounds from TCM through network efficiency and network flux, especially

multi-target candidate drugs. Finally, comparing with target-based virtual screening, it could simulate drug actions in the context of pathway network, and bridge the gap between drug-target interaction and the systematic behavior of cells (phenotype). Thus, it would be helpful to screen lead compounds in early-phase drug discovery and improve the success rates in last stage drug development. In addition, it could be applied to explore the molecular mechanism of TCM.

Acknowledgments

The authors gratefully acknowledge financial support from the National Science and Technology Major Project 'Key New Drug Creation and Manufacturing Program' (Grant No. 2013ZX09402203, 2012ZX09501001-004 and 2013ZX09402202). The calculations were performed on TianHe-1(A) at National Supercomputer Center in Tianjin, PR China. The authors gratefully acknowledge their support from National Supercomputer Center.

Author Contributions

W. Xiao, X.J. Xu and L.R. Chen conceived the study. X. Z. Zhang, J.Y. Gu and F. Luo constructed pathway network, collected compounds and performed computational analyses. X. Z. Zhang, Y. M. Ma and Z. Z. Su carried out *in vitro* assays with the help of L. Cao, Z. Z. Wang, N. Li, G. Yuan. X. Z. Zhang and J.Y. Gu interpreted the results and wrote the manuscript.

References

1. I. Khanna, *Drug Discov Today*, 2012, 17, 1088-1102.
2. I. Kola and J. Landis, *Nat Rev Drug Discov*, 2004, 3, 711-715.
3. D. C. Swinney, *Clin Pharmacol Ther*, 2013, 93, 299-301.

4. W. Zheng, N. Thorne and J. C. McKew, *Drug Discov Today*, 2013, 18, 1067-1073.
5. J. B. Brown and Y. Okuno, *Chem Biol*, 2012, 19, 23-28.
6. Y. Li and P. Agarwal, *PLoS One*, 2009, 4, e4346.
7. P. I. Wang and E. M. Marcotte, *J Proteomics*, 2010, 73, 2277-2289.
8. J. Loscalzo, I. Kohane and A. L. Barabasi, *Mol Syst Biol*, 2007, 3, 124.
9. F. Barrenas, S. Chavali, P. Holme, R. Mobini and M. Benson, *PLoS One*, 2009, 4, e8090.
10. A. Mitsos, I. N. Melas, P. Siminelakis, A. D. Chairakaki, J. Saez-Rodriguez and L. G. Alexopoulos, *PLoS Comput Biol*, 2009, 5, e1000591.
11. Q. Li, X. Li, C. Li, L. Chen, J. Song, Y. Tang and X. Xu, *PLoS One*, 2011, 6, e14774.
12. J. Gu, Q. Li, L. Chen, Y. Li, T. Hou, G. Yuan and X. Xu, *Evid Based Complement Alternat Med*, 2013, 2013, 425707.
13. A. I. Ivanov and A. A. Romanovsky, *Front Biosci*, 2004, 9, 1977-1993.
14. L. Chen, G. Yang and T. Grosser, *Prostaglandins Other Lipid Mediat*, 2013, 104-105, 58-66.
15. E. Pecchi, M. Dallaporta, A. Jean, S. Thirion and J.-D. Troadec, *Physiology & Behavior*, 2009, 97, 279-292.
16. D. M. Aronoff and E. G. Neilson, *The American Journal of Medicine*, 2001, 111, 304-315.
17. G. Zhang, J. Zhao, L. He, S. Yan, Z. Zhuo, H. Zheng, Y. Mu, S. Li, X. Zhang, J. Huang, X. Li, J. Liu, H. Wan, C. Wei and W. Xiao, *Journal of traditional Chinese medicine = Chung i tsa chih ying wen pan / sponsored by All-China Association of Traditional Chinese Medicine, Academy of Traditional Chinese Medicine*, 2013, 33, 733-742.
18. H. Xu, Y. Wang and N. Liu, *Pharmacy World & Science*, 2009, 31, 458-463.
19. X. Li, X. Zhang, J. Ding, Y. Xu, D. Wei, Y. Tian, W. Chen, J. Huang, T. Wen and S. Li, *Evidence-Based Complementary and Alternative Medicine*, 2014, 2014, 7.
20. M. R. Waterfield, M. Zhang, L. P. Norman and S. C. Sun, *Mol Cell*, 2003, 11, 685-694.
21. T. Gantke, S. Sriskantharajah and S. C. Ley, *Cell Res*, 2011, 21, 131-145.
22. Y. Yang, T. Yu, H. J. Jang, S. E. Byeon, S. Y. Song, B. H. Lee, M. H. Rhee, T. W. Kim, J. Lee, S. Hong and J. Y. Cho, *J Ethnopharmacol*, 2012, 139, 616-625.
23. C. Tsatsanis, A. Androulidaki, M. Venihaki and A. N. Margioris, *Int J Biochem Cell Biol*, 2006, 38, 1654-1661.
24. B. Beutler, *Curr Opin Immunol*, 2000, 12, 20-26.

25. Y. J. Kang, B. A. Wingerd, T. Arakawa and W. L. Smith, *Journal of Immunology*, 2006, 177, 8111-8122.

26. A. G. Eliopoulos, C. D. Dumitru, C. C. Wang, J. H. Cho and P. N. Tsichlis, *Embo Journal*, 2002, 21, 4831-4840.

27. Y. C. Lu, W. C. Yeh and P. S. Ohashi, *Cytokine*, 2008, 42, 145-151.

28. L. Matthews, G. Gopinath, M. Gillespie, M. Caudy, D. Croft, B. de Bono, P. Garapati, J. Hemish, H. Hermjakob, B. Jassal, A. Kanapin, S. Lewis, S. Mahajan, B. May, E. Schmidt, I. Vastrik, G. Wu, E. Birney, L. Stein and P. D'Eustachio, *Nucleic Acids Res*, 2009, 37, D619-622.

29. M. Kanehisa, S. Goto, M. Furumichi, M. Tanabe and M. Hirakawa, *Nucleic Acids Res*, 2010, 38, D355-360.

30. X. Jiang, K. Kumar, X. Hu, A. Wallqvist and J. Reifman, *Chem Cent J*, 2008, 2, 18.

31. H. Park, J. Lee and S. Lee, *Proteins*, 2006, 65, 549-554.

32. Y.-J. Li, Z.-Z. Wang, Y.-A. Bi, G. Ding, L.-S. Sheng, B. Musselman, C.-F. Zhang, J. Chen and W. Xiao, *Analytical Methods*, 2013, 5, 7081-7089.

33. Y. J. Li, Z. Z. Wang, Y. A. Bi, G. Ding, L. S. Sheng, J. P. Qin, W. Xiao, J. C. Li, Y. X. Wang and X. Wang, *Rapid communications in mass spectrometry : RCM*, 2012, 26, 1377-1384.

34. K. Natarajan, S. Singh, T. R. Burke, D. Grunberger and B. B. Aggarwal, *Proceedings of the National Academy of Sciences of the United States of America*, 1996, 93, 9090-9095.

35. A. Kumar and U. Bora, *international journal of Medicinal Chemistry*, 2012, 2012, 1-8.

36. V. Agoston, P. Csermely and S. Pongor, *Phys Rev E Stat Nonlin Soft Matter Phys*, 2005, 71, 051909.

37. P. Csermely, V. Agoston and S. Pongor, *Trends Pharmacol Sci*, 2005, 26, 178-182.

38. P. V. Missiuro, K. Liu, L. Zou, B. C. Ross, G. Zhao, J. S. Liu and H. Ge, *PLoS Comput Biol*, 2009, 5, e1000350.

39. D. Y. Cho, Y. A. Kim and T. M. Przytycka, *PLoS Comput Biol*, 2012, 8, e1002820.

40. F. Luo, J. Gao, Y. H. Cheng, W. Cui and M. J. Ji, *Acta Physico-Chimica Sinica*, 2012, 28, 2191-2201.

41. M. E. Smoot, K. Ono, J. Ruscheinski, P.-L. Wang and T. Ideker, *Bioinformatics*, 2011, 27, 431-432.

42. A.-L. Barabási, *Science*, 2009, 325, 412-413.

43. X. Xu, J. W. Luo and Y. T. Gu, *International Journal of Bifurcation and Chaos*, 2012, 22, 1250281.

44. J. Stelling, U. Sauer, Z. Szallasi, F. J. Doyle and J. Doyle, *Cell*, 2004, 118, 675-685.

45. H. Kitano, *Nature Reviews Drug Discovery*, 2007, 6, 202-210.

46. M. P. Joy, A. Brock, D. E. Ingber and S. Huang, *J Biomed Biotechnol*, 2005, 2005, 96-103.

47. W. C. Hwang, A. Zhang and M. Ramanathan, *Clin Pharmacol Ther*, 2008, 84, 563-572.

48. S. Netotea and S. Pongor, *Cellular Immunology*, 2006, 244, 80-83.

49. R. Heilker, M. Wolff, C. S. Tautermann and M. Bieler, *Drug Discovery Today*, 2009, 14, 231-240.

50. T. Furuyashiki and S. Narumiya, *Current Opinion in Pharmacology*, 2009, 9, 31-38.

51. V. Konya, G. Marsche, R. Schuligoi and A. Heinemann, *Pharmacol Ther*, 2013, 138, 485-502.

52. J. Y. Park, M. H. Pillinger and S. B. Abramson, *Clinical Immunology*, 2006, 119, 229-240.

53. H.-J. Huang, H. W. Yu, C.-Y. Chen, C.-H. Hsu, H.-Y. Chen, K.-J. Lee, F.-J. Tsai and C. Y.-C. Chen, *Journal of the Taiwan Institute of Chemical Engineers*, 2010, 41, 623-635.

54. X. J. Yao, Z. Q. Ding, Y. F. Xia, Z. F. Wei, Y. B. Luo, C. Feleder and Y. Dai, *International Immunopharmacology*, 2012, 14, 454-462.

55. W. S. Yang, D. Jeong, Y. S. Yi, J. G. Park, H. Seo, S. H. Moh, S. Hong and J. Y. Cho, *Mediators of Inflammation*, 2013, 2013, 518183.

56. B. Kaminska, *Biochim Biophys Acta*, 2005, 1754, 253-262.